Multispectral Statistical Geometrical Features for Texture Analysis and Classification

Christian Münzenmayer[1], Heiko Volk[1], Dietrich Paulus[2], Florian Vogt[3], and Thomas Wittenberg[1]

[1] Fraunhofer Institut für Integrierte Schaltungen
Am Wolfsmantel 33, D-91058 Erlangen
{mzn,vlk,wbg}@iis.fhg.de
[2] Institut für Computervisualistik, Universität Koblenz-Landau
Universitätsstraße 1, D-56070 Koblenz
paulus@uni-koblenz.de
[3] Lehrstuhl für Mustererkennung, Universität Erlangen-Nürnberg
Martensstr. 3, D-91058 Erlangen
vogt@informatik.uni-erlangen.de

Abstract

In this paper we present a new approach for color texture classification which extends the gray level statistical geometrical features (SGF) proposed by Chen. This feature extractor computes 16 statistical measures based on the geometrical properties of connected regions in a series of binary images derived from the gray scale image.

We propose intra-plane, inter-plane and the so-called non-linear H'V features as extensions into the color domain. Improvements in classification rates up to 20% by using our multispectral statistical geometrical features compared with the original gray scale features and color histograms have been achieved.

1 Introduction

Various solutions in medical and industrial applications make use of texture algorithms for classification of structured surfaces. Examples from medical applications include microscopic images of cells, tissue and endoscopic images of mucous membranes of e.g. the larynx or intestine. Industrial applications are the decor of furniture or woodcut surfaces in the quality control of sawmills.

With more processing power at hand and new problems arising in industrial and medical applications, the fusion of color and texture approach promises better classification performance.

Several different approaches to color texture are described in literature already (e.g. [PH95, Lak98, JH98]). In this paper we will describe a new approach based on the statistical geometrical features (SGF) by Chen [CNT95].

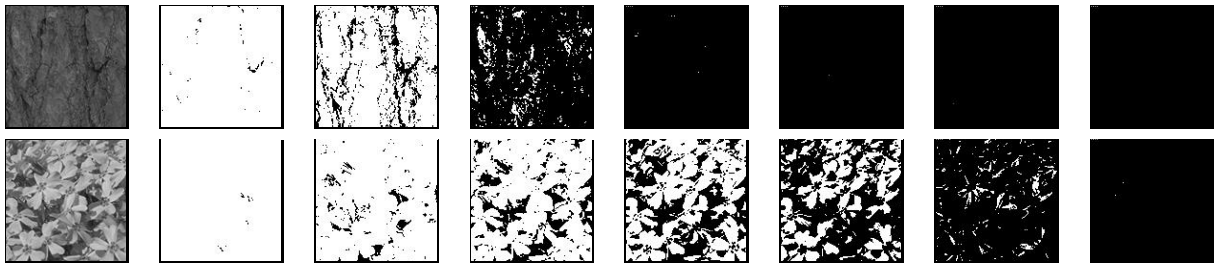

Figure 1: Chen binarization example. Different thresholds α_i are applied to the gray level version of a bark image (top) and a flower image (bottom) with $\alpha_0 = \Delta\alpha = 32$ resulting in $L_{\text{Bins}} = 7$ binary images.

α_0	$\Delta\alpha$	G	L_{Bins}
4	4	256	63
8	8	256	31
16	16	256	15
32	32	256	7

Table 1: Example SGF binarization levels depending on initial threshold α_0, the step size $\Delta\alpha$ and the number of gray levels G. More binarization levels result in higher runtime complexity.

2 Statistical Geometrical Features

2.1 Gray level features

The statistical geometrical features algorithm presented by Chen et al. [CNT95] computes 16 statistical measures based on the geometrical properties of connected regions in a series of binary images. These binary images are produced by thresholding operations on the gray scale image. Geometrical properties like the number of connected regions and their irregularity together with their statistics (mean, standard deviation) describing the stack of binary images are used. Figure 2(a) gives an overview of the feature extraction process. For an image $I(x, y)$ with G gray levels a binary image $I_{\text{B}\alpha}(x, y)$ can be obtained by thresholding with a threshold value $\alpha \in [1; G-1]$ resulting in

$$I_{\text{B}\alpha}(x, y) = \begin{cases} 1 & \text{if } I(x, y) \geq \alpha, \\ 0 & \text{otherwise.} \end{cases} \tag{1}$$

A sample series of binary images is shown in Figure 1. In this work a reduced set of binarization levels is used which is parameterized by an initial threshold α_0 and a step size $\Delta\alpha$. The series of thresholds is obtained by $\alpha_i = \alpha_0 + i\Delta\alpha$, with $i = 0, \ldots, L_{\text{Bins}} - 1$. Typical values for these parameters are shown in Table 1. The number of binary images L_{Bins} should be as small as possible, weighting classification performance against runtime complexity.

Within each binary image, connected regions employing 4-neighborhoods are extracted from the 1-valued and 0-valued pixels respectively. Details regarding the definitions and a recursive algorithm to find those regions can be found in the appendix of [CNT95] and

Feature	Equation
Max value	$g_{max} = \max_{\alpha} g(\alpha)$
Average value	$\mu_g = \frac{1}{L_{\text{Bins}}} \sum_{\alpha} g(\alpha)$
Sample mean	$\mu_{g\alpha} = \frac{1}{\sum_{\alpha} g(\alpha)} \sum_{\alpha} \alpha g(\alpha)$
Sample S.D.	$\sigma_{g\alpha} = \sqrt{\frac{1}{\sum_{\alpha} g(\alpha)} \sum_{\alpha} (\alpha - \mu_{g\alpha})^2 g(\alpha)}$

Table 2: Statistical features which are computed on the geometrical properties $g(\alpha) \in \{\text{NOC}_0(\alpha), \text{NOC}_1(\alpha), \overline{\text{IRGL}}_0(\alpha), \overline{\text{IRGL}}_1(\alpha)\}$ according to [CNT95].

will not be elaborated further in this work. Using these regions, the number of connected regions (NOC) of k-valued pixels with $k \in \{0, 1\}$ is denoted by $\text{NOC}_k(\alpha)$. The total number of k-valued pixels within a region R_i will be called $\text{NOP}_k(i, \alpha) = |R_i|$ here. In addition the irregularity (IRGL) of each region R_i is defined as

$$\text{IRGL}_k(i, \alpha) = \frac{1 + \sqrt{\pi} \max\limits_{j \in R_i} \sqrt{(x_j - \overline{x}_i)^2 + (y_j - \overline{y}_i)^2}}{\sqrt{|R_i|}} - 1, \tag{2}$$

where

$$\overline{x}_i = \frac{\sum_{j \in R_i} x_j}{|R_i|}, \overline{y}_i = \frac{\sum_{j \in R_i} y_j}{|R_i|} \tag{3}$$

are the centres of mass of the respective region. It is proportional to the maximal distance of a border point from the centre of mass. Now, for every threshold α the weighted mean irregularity of regions within the corresponding binary image $I_{\text{B}\alpha}(x, y)$ is computed as

$$\overline{\text{IRGL}}_k(\alpha) = \frac{\sum_i \text{NOP}_k(i, \alpha) \text{IRGL}_k(i, \alpha)}{\sum_i \text{NOP}_k(i, \alpha)} \tag{4}$$

where the weighting is done by the number of pixels $\text{NOP}_k(i, \alpha)$ within each region R_i. From the four functions $\text{NOC}_0(\alpha)$, $\text{NOC}_1(\alpha)$, $\overline{\text{IRGL}}_0(\alpha)$ and $\overline{\text{IRGL}}_1(\alpha)$, Chen obtains four statistical measures (see Table 2). This leads to a total of 16 features which are characteristic for different textures.

2.2 Intra-plane Features

The SGF features will first be applied to each plane of a linear color space independently yielding the *intra-plane* features. These features will be concatenated to the complete feature vector with 48 entries for an RGB image (Figure 2(b)). We will also use these features on a color difference representation which was adopted from [PV00]:

$$I_1 = \frac{R + G + B}{3}, \quad I_2 = \frac{R - B}{2} + 128, \quad I_3 = \frac{2G - R - B}{4} + 128. \tag{5}$$

The I1I2I3 conversion yields an intensity and two color difference signals, thus decorrelating the image planes and making classification improvements more likely.

2.3 Inter-plane Features

To capture *inter-plane* dependencies, combinations of color planes have to be used. The three fundamental boolean operations AND, OR and XOR present themselves as an obvious solution to combine the binary stacks from different image planes (Figure 2(c)). For a color image $\vec{I}(x,y)$ with channel indices $p \neq q$, *inter-plane* binary images $I_{\mathrm{B}\alpha}^{(pq)}(x,y)$ can be obtained by

$$I_{\mathrm{B}\alpha}^{(pq)}(x,y) = I_{\mathrm{B}\alpha}^{(p)}(x,y) \odot I_{\mathrm{B}\alpha}^{(q)}(x,y), \tag{6}$$

$$I_{\mathrm{B}\alpha}^{(p)}(x,y) = \begin{cases} 1 & \text{if } I^{(p)}(x,y) \geq \alpha, \\ 0 & \text{otherwise,} \end{cases} \tag{7}$$

where $\odot$ is one of the boolean operations AND ($\wedge$), OR ($\vee$) and XOR ($\oplus$) and $p, q \in \{R, G, B\}$. This leads to three binary images or masks $I_{\mathrm{B}\alpha}^{(pq)}$ for feature calculation as in the *intra-plane* method. Feature vectors are concatenated afterwards yielding 48 features.

2.4 Non-Linear H'V Features

Instead of the highly correlated and symmetric RGB color space, the HSV (hue, saturation, value) color model will be used as well. For small saturation values the hue is highly sensible to sensor noise in the image. Therefore, we use the information from the H channel only if a certain saturation threshold $S_{\min}$ is exceeded and otherwise set H to an arbitrary but constant value:

$$H' = \begin{cases} H & \text{if } S \geq S_{\min}, \\ 0 & \text{otherwise.} \end{cases} \tag{8}$$

Sample images of the hue channel after this thresholding-operation are shown in Figure 3. Features can then be calculated on the H' and the V plane individually which we will call *nonlinear H'V* features (Figure 2(d)).

It should be noted that this constitutes no double thresholding as the hue channel H is thresholded regarding the corresponding saturation value S of a certain pixel. For building the binary stack on the H'V space each channel will be processed individually.

3 Experiments and Results

To validate our newly defined texture features we used four different color image sets. As a well known academic set we chose 32 images from the *VisTex* database [Vg95]. We selected 10 disjoint regions of interest (ROI) in each image for classification experiments. The *BarkTex* database which contains 414 images of bark from six different types of trees constitues another relatively difficult classification problem [Lak98]. A more practical image set was compiled from a project for cancer prevention by screening of *cervical cells* where healthy cells should be discriminated from precancerous cells by their nuclues structure. It is a known fact from biology that precancerous dysplasia cause changes in the chromatin structure of the nuclei. For this work we used 53 healthy reference

Table 3: Validation image sets from the VisTex [Vg95] and BarkTex [Lak98] databases. The cell images are compiled from a cancer prevention project and the Wood images contains different wood cut images.

Name	Classes	Images	Size	ROI-size	ROI/img	ROI/class	#ROIs
VisTex	32	32	512x512	64x64	10	10	320
BarkTex	6	414	256x384	64x64	4	272	1624
Cells	2	37	1000x700	32x32	-	53	106
Wood	7	208	128x128	128x128	1	-	208

Table 4: Classification results using leaving-one-out classification scheme. Recognition rates are shown in % for threshold parameters α_0 and $\Delta\alpha$ which lead to the best gray scale rate.

Set	$\Delta\alpha$	α_o	Gray	Histo	Intra	I1I2I3	Inter	Op	H'V	S_{min}
VisTex	8	8	93%	95%	97%	**99%**	**99%**	XOR	97%	50
BarkTex	4	4	65%	77%	80%	83%	**85%**	XOR	84%	0
Cells	4	4	88%	90%	**91%**	80%	87%	XOR	87%	50
Wood	4	4	67%	58%	67%	**75%**	74%	OR	71%	0

and 53 dysplastic cell nuclei. A sample from industrial image processing is the *Wood* image database which contains images from wood cut surfaces with seven different classes. Among other these include normal wood, knotholes and bark margins.

Classification results were obtained by applying the leaving-one-out classification scheme with a nearest neighbor classifier using the L2 norm. All features were normalized to mean $\mu = 0$ and standard deviation $\sigma = 1$. The proposed color texture features are evaluated in the context of their gray scale counterpart as well as color histogram features, being the two extreme references for texture and color.

Recognition rate and runtime performance are influenced by the thresholding stepsize $\Delta\alpha$ and start point α_0 which determine the number of binary images L_{Bins}. In general more binary images lead to better classification results but slow done feature calculation.

Three thresholding settings were used in the experiments with $\Delta\alpha = \alpha_0 \in \{4, 8, 16\}$. A summary presenting the best results was compiled into Table 4. If several recognition rates have been equal, the one with a larger threshold step $\Delta\alpha$ was selected because less binary images L_{Bins} are produced.

Using these parameters, the proposed intra- and inter-plane features were applied. Classification results are shown in Table 4 with the best result marked in bold face. Column *Op* shows the binary operation for inter-plane features which lead to best recognition rates. For each experiment the AND, OR and XOR operation were used. Similarly, the column S_{min} shows the thresholds which lead to the best recognition rates for the H'V features. For each experiment values of $S_{min} \in \{0, 25, 50, 100, 150, 200\}$ were applied.

4 Discussion

In this paper we presented four different approaches to extend the SGF for multispectral images. Classification results improved significantly for three of the used image sets as can be seen in Table 4. The intra-plane features in I1I2I3 and the inter-plane features

using the XOR operation outperformed intra-plane features in RGB and non-linear H'V features as well as the gray level algorithm and color histograms.

In contrast, recognition rates for the Cervix cell nuclei which have a quite gray appearance improved only slightly. Therefore, we must conclude that some applications might still be solved in the gray level domain alone and a case by case decision in favor or against color texture is necessary.

Compared with the *intra-* and *inter-plane* method the non-linear H'V features achieve similar classification performance using less features (32 instead of 48). In two cases (see Table 4) a threshold of $S_{min} = 0$ lead to similar results as with a treshold $S_{min} > 0$. Therefore, it seems that in some cases hue and value alone might contain enough information for satisfying results.

In the other cases, however, finding appropriate saturation thresholds adds another degree of freedom to the already difficult task of finding optimal parameter settings for real-world applications.

For practical applications we suggest the *intra-plane* features after I1I2I3-conversion and the *inter-plane* features with an *XOR* operation. Future work will focus on the application of these operators to irregularly bounded regions, normalization of the SGF regarding ROI size and further evaluation in the context of image segmentation tasks together with large image sets.

References

[CNT95] Y. Q. Chen, M. S. Nixon, and D. W. Thomas. Statistical geometrical features for texture classification. *Pattern Recognition*, 28(4):537–552, September 1995.

[JH98] A. Jain and G. Healey. A Multiscale Representation Including Opponent Color Features for Texture Recognition. *IEEE Transactions on Image Processing*, 7(1):124–128, January 1998.

[Lak98] R. Lakmann. *Statistische Modellierung von Farbtexturen.* PhD thesis, Universität Koblenz-Landau, Koblenz, 1998.

[PH95] D. K. Panjwani and G. Healey. Markov random field models for unsupervised segmentation of textured color images. *IEEE Transactions on Pattern Analysis and Machine Intelligence*, 17(10):939–954, October 1995.

[PV00] K. N. Plataniotis and A. N. Venetsanopoulos. *Color Image Processing and Applications.* Springer-Verlag, Berlin, 1. edition, 2000.

[Vg95] MIT Media Laboratory Vision and Modeling group. Vistex vision texture database, http://whitechapel.media.mit.edu/vismod/imagery/visiontexture, 1995.

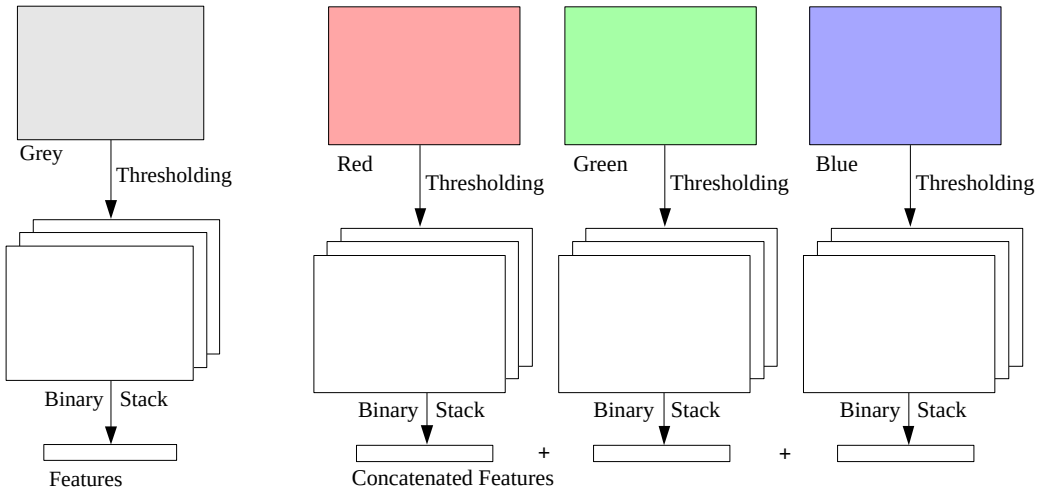

(a) Gray (b) Intra-plane

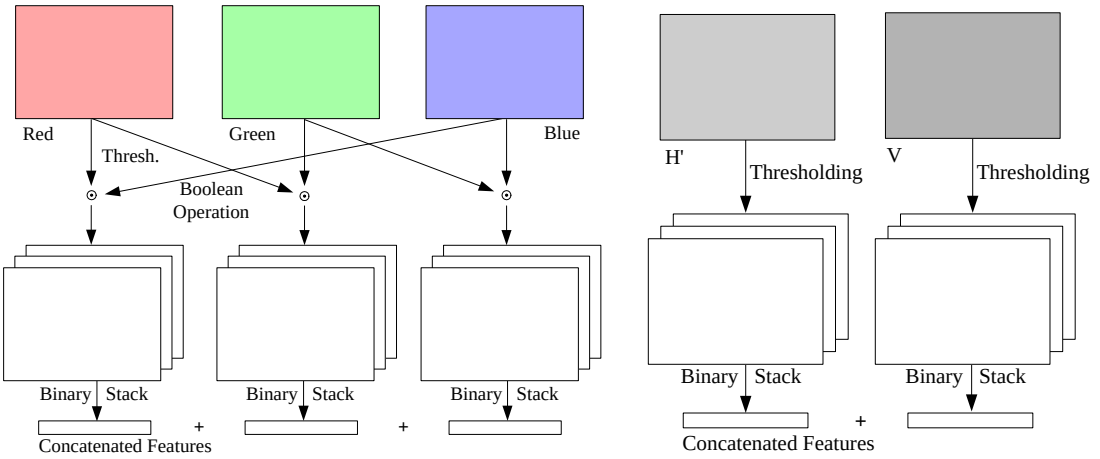

(c) Inter-plane (d) Non-linear H'V

Figure 2: Gray level version and different color extensions to the statistical geometrical features.

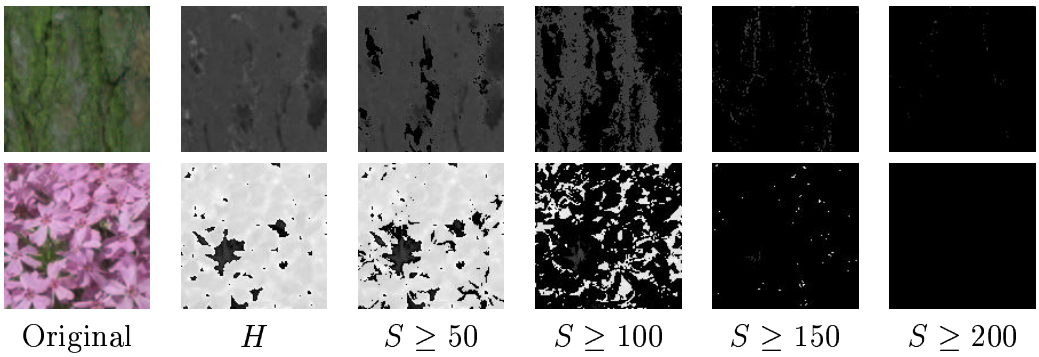

Figure 3: Thresholding in hue channel of ps_022 (top) and Flowers.0002 image (bottom).

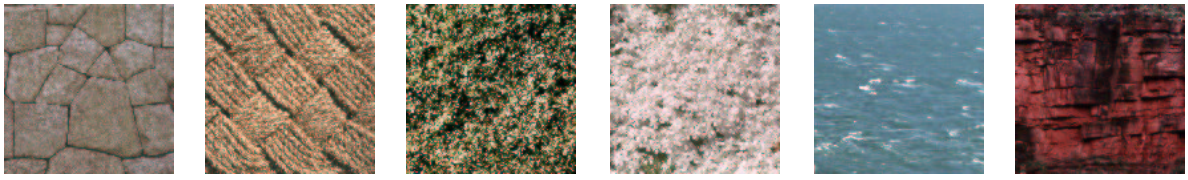

Figure 4: Sample 64×64 regions from VisTex images.

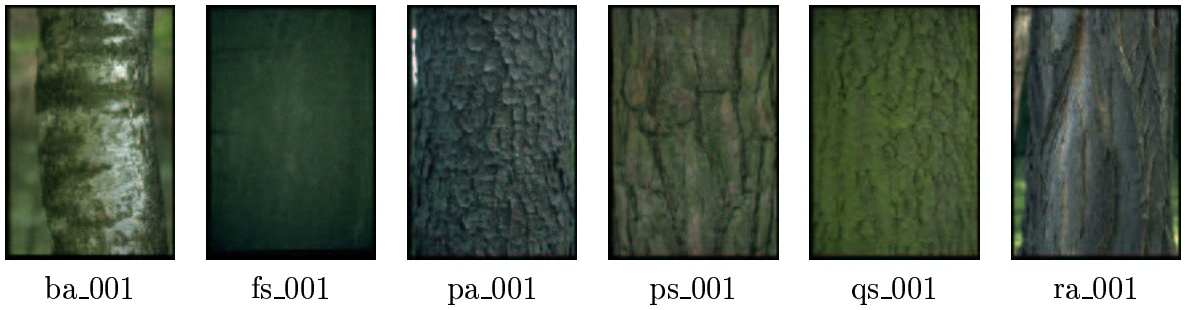

Figure 5: BarkTex sample images with one representative per class.

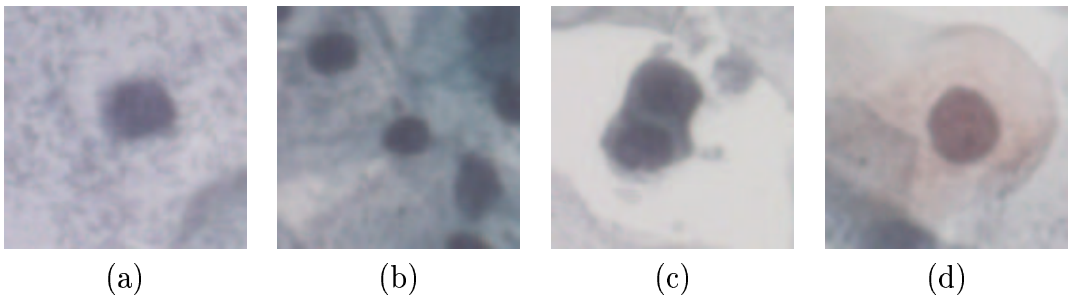

Figure 6: Sample cell images from two different samples with healthy (a+b) and dysplastic (c+d) cell nucleus in the center.

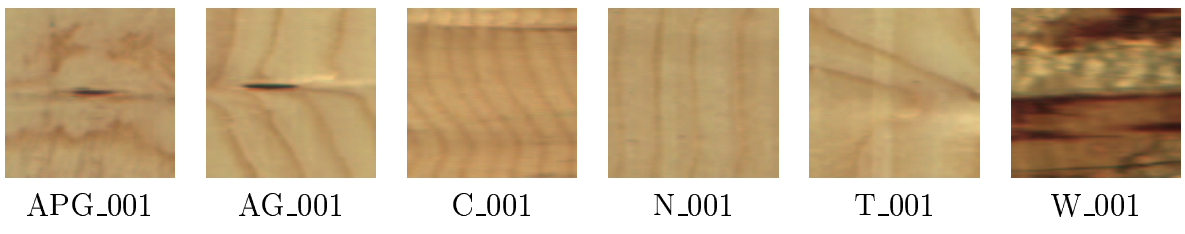

Figure 7: Wood sample images of size 128×128.